Impact of large-scale tides on cosmological distortions via redshift-space power spectrum

Kazuyuki Akitsu[1,2] and Masahiro Takada[1]

[1]*Kavli Institute for the Physics and Mathematics of the Universe (WPI), The University of Tokyo Institutes for Advanced Study (UTIAS), The University of Tokyo, Chiba 277-8583, Japan*
[2]*Department of Physics, Graduate School of Science, The University of Tokyo, 7-3-1 Hongo, Bunkyo-ku, Tokyo 113-0033, Japan*

(Received 9 November 2017; published 26 March 2018)

Although large-scale perturbations beyond a finite-volume survey region are not direct observables, these affect measurements of clustering statistics of small-scale (subsurvey) perturbations in large-scale structure, compared with the ensemble average, via the mode-coupling effect. In this paper we show that a large-scale tide induced by scalar perturbations causes apparent anisotropic distortions in the redshift-space power spectrum of galaxies in a way depending on an alignment between the tide, wave vector of small-scale modes and line-of-sight direction. Using the perturbation theory of structure formation, we derive a *response* function of the redshift-space power spectrum to large-scale tide. We then investigate the impact of large-scale tide on estimation of cosmological distances and the redshift-space distortion parameter via the measured redshift-space power spectrum for a hypothetical large-volume survey, based on the Fisher matrix formalism. To do this, we treat the large-scale tide as a signal, rather than an additional source of the statistical errors, and show that a degradation in the parameter is restored if we can employ the prior on the rms amplitude expected for the standard cold dark matter (CDM) model. We also discuss whether the large-scale tide can be constrained at an accuracy better than the CDM prediction, if the effects up to a larger wave number in the nonlinear regime can be included.

DOI: 10.1103/PhysRevD.97.063527

I. INTRODUCTION

A number of wide-area and deep galaxy surveys are ongoing and planned, aimed at revealing the nature of primordial perturbations, the physics in the early universe, the curvature of the universe, the origin of cosmic acceleration as well as weighing neutrino mass via a measurement of large-scale structure probes such as weak gravitational lensing, baryon acoustic oscillations (BAO), galaxy clustering and redshift-space distortions (e.g., [1–3]). In particular, when combined with a high-precision measurement of cosmic microwave background (CMB) anisotropies, large-scale structure probes allow one to study the time evolution of perturbations over cosmic time, which is sensitive to the aforementioned physics and cosmological parameters (e.g. [4]).

The linear perturbation theory can accurately describe the time evolution of large-scale perturbations in structure formation, based on the standard Λ and cold dark matter dominated cosmology with Gaussian adiabatic initial conditions (hereafter ΛCDM) [5], which successfully reproduces the high-precision measurements of CMB anisotropies, yielding stringent constraints on the cosmological parameters [6]. The linear theory, however, breaks down in the late-time universe, which is relevant for galaxy surveys, because the *nonlinear* structure formation induces a mode coupling between different Fourier modes of the perturbations owing to the nature of nonlinear, long-range gravity ([7,8] for a thorough review). As a result, the power spectrum of large-scale structure probes, measured from a galaxy survey, no longer carries the full information unlike CMB anisotropies, and the statistical properties display a substantial non-Gaussianity that is described by higher-order correlation functions [9]. A better understanding of the nonlinear structure formation is thus required in order to attain the full potential of wide-area galaxy surveys.

Even though a wide-area galaxy survey is to cover a huge cosmological volume, there is an unavoidable uncertainty in the statistical analysis of large-scale structure probes arising due to finiteness of the survey volume as well as the nonlinear mode coupling, as studied in Refs. [10–33]. A finite-volume survey realization is generally embedded into large-scale perturbations that are not directly observable—which we hereafter call "super-survey modes" [10,26]. Although the super-survey modes have small amplitudes and are well in the linear regime for a wide-area galaxy survey, it causes a non-negligible effect on small-scale perturbations due to the nonlinear mode coupling, compared with the statistical accuracies in measurements of the small-scale perturbations. Hence, it is necessary to include

the effects in the cosmological analysis (e.g. [34]) in order not to have any biased estimation in cosmological parameters as well as not to have too optimistic cosmological constraints.

The physical effects of super-survey modes on structure formation at equal time arise from the second-derivative tensor of the large-scale gravitational field due to the equivalence principle [16,31]. The tensor is decomposed into two modes: the trace part or large-scale density contrast and the traceless tensor which we hereafter call the large-scale tide. While the effect of large-scale density contrast is well studied in previous studies (e.g. [10]), the effect of large-scale tide has not been fully studied, except for some studies [19,27,30–32,35]. In our previous study [31], we showed that a large-scale tide causes an anisotropic clustering in the redshift-space power spectrum. The effect mimics the redshift-space distortion effect [36,37] arising from the peculiar velocities of large-scale structure tracers as well as the Alcock-Paczynski (AP) distortion [38–40] arising from the use of an incorrect cosmological model in the clustering analysis. Yet we studied only the partial effect, the effect of the large-scale tide on the real-space clustering; in other words, we did not include the effect of large-scale tide on redshift-space distortion as well as a modulation in the mapping between real- and redshift-space distributions of galaxies.

Hence, the purpose of this paper is to study the effects of large-scale tide on the redshift-space power spectrum, based on the perturbation theory [7]. To do this, we derive *response* functions of the redshift-space power spectrum to super-survey modes, which describe how the super-survey modes in a given survey realization affect the redshift-space power spectrum as a function of wave vector $\mathbf{k}$ and the line-of-sight direction, say $\hat{\mathbf{n}}$, relative to the large-scale tide. We then discuss the impact of the tide on estimation of cosmological distances and the redshift-space distortion parameter via a measurement of the redshift-space power spectrum for a hypothetical large-volume galaxy survey, using the Fisher matrix formalism.

The rest of this paper is organized as follows. In Sec. II, we define the super-survey modes and introduce its isotropic component and anisotropic components. In Sec. III, we derive the response function of the redshift-space power spectrum to super-survey modes by considering the squeezed-limit bispectrum that is a cross-correlation of the super-survey modes with the redshift-space power spectrum estimator. In Sec. IV, we study the impact of the super-survey modes on cosmological parameter estimation from a measurement of the redshift-space power spectrum, including the AP test, based on the Fisher information matrix analysis. Section V is devoted to the discussion. In the Appendix, we give expressions for the multipole expansion of the redshift-space power spectrum in the presence of the super-survey modes.

II. PRELIMINARIES

The redshift-space density field of galaxies observed in a finite-volume survey region can be expressed, using the survey window function $W(\mathbf{x})$, following the formulation in Ref. [10]:

$$\delta_{sW}(\mathbf{x}) = W(\mathbf{x})\delta_s(\mathbf{x}), \tag{1}$$

where $\delta_{sW}(\mathbf{x})$ is the observed density field, $\delta_s(\mathbf{x})$ is the underlying true density field in redshift space, and the survey window is defined in that $W(\mathbf{x}) = 1$ if $\mathbf{x}$ is inside the survey geometry, and otherwise $W(\mathbf{x}) = 0$. Throughout this paper we assume that a survey window is given in the background comoving coordinate. The survey volume is defined in terms of the survey window as

$$V_W = \int \mathrm{d}^3\mathbf{x} W(\mathbf{x}). \tag{2}$$

In the following we assume a well-behaved survey window for simplicity; we do not consider effects of masks that might cause additional mode-coupling between high-k modes in the observed power spectrum. The Fourier transform of the density field is

$$\tilde{\delta}_{sW}(\mathbf{k}) = \int \frac{\mathrm{d}^3\mathbf{q}}{(2\pi)^3}\tilde{W}(\mathbf{q})\tilde{\delta}_s(\mathbf{k}-\mathbf{q}), \tag{3}$$

where quantities with tilde symbol such as $\tilde{\delta}_s(\mathbf{k})$ are their Fourier transforms. The survey window $\tilde{W}(\mathbf{k})$ is non-vanishing for $k \ll 1/L$, while $\tilde{W}(\mathbf{k}) \simeq 0$ for $k \gg 1/L$, where L is a typical scale of the survey volume. The above equation explicitly shows that the Fourier transform of the observed field has a contribution from long-wavelength modes beyond a survey window, i.e. super-survey modes, via a convolution with the survey window.

Redshift-space distortion (RSD) effect due to peculiar velocities of galaxies causes a modulation in the observed clustering pattern of galaxies along the line-of-sight direction. Thus the RSD effect violates statistical isotropy of the galaxy distribution. For this reason the monopole power spectrum, measured by the azimuthal-angle average of power spectrum over $\mathrm{d}\Omega_{\mathbf{k}}$, cannot carry the full information. Instead a standard approach to quantify the redshift-space clustering of galaxies is using the power spectrum, given as a function of the three-dimensional wave vector $\mathbf{k}$. An estimator of the power spectrum for a given survey window is defined as

$$\hat{P}_s(\mathbf{k}) \equiv \frac{1}{V_W}\int_{\mathbf{k}'\in\mathbf{k}} \frac{\mathrm{d}^3\mathbf{k}'}{V_{\mathbf{k}}}\tilde{\delta}_{sW}(\mathbf{k})\tilde{\delta}_{sW}(-\mathbf{k}), \tag{4}$$

where the integration is done over a volume element around the mode $\mathbf{k}$ (a target wave vector for the power spectrum measurement), and $V_{\mathbf{k}}$ is the volume: $V_{\mathbf{k}} \equiv \int_{\mathbf{k}'\in\mathbf{k}} \mathrm{d}^3\mathbf{k}'$. If a

bin width around the bin $\mathbf{k}$ is given by Δk, $V_{\mathbf{k}} \simeq (\Delta k)^3$. This definition does *not* include an angle average of $\mathrm{d}\Omega_{\mathbf{k}}$, unlike a definition of the monopole power spectrum. Hence, at this point, the redshift-space power spectrum $\hat{P}_s(\mathbf{k})$ is given as a function of the three-dimensional vector, $\mathbf{k}$. A standard method usually further assumes the statistical isotropy in the two-dimensional plane (angular direction) perpendicular to the line-of-sight direction, and then uses the power spectrum given as a function of *two-dimensional* vector $(k_\parallel, k_\perp)$, where $k_\parallel$ is the line-of-sight direction component of $\mathbf{k}$, $\mathbf{k}_\perp$ is the vector in the two-dimensional plane perpendicular to the line-of-sight direction, and $k_\perp = |\mathbf{k}_\perp|$. Here we do not introduce the angle average over $\mathrm{d}\varphi_{\mathbf{k}_\perp}$ in the perpendicular plane, where $\varphi_{\mathbf{k}_\perp}$ is defined via $\mathbf{k}_\perp = k_\perp(\cos\varphi_{\mathbf{k}}, \sin\varphi_{\mathbf{k}})$, and keep the general definition of $\hat{P}_s(\mathbf{k})$ because the large-scale tide generally causes anisotropic distortions in the redshift-space clustering pattern of galaxies in all three-dimensional directions (also see Ref. [41], for the similar discussion).

Given the definition of the redshift-space power spectrum,

$$\langle \tilde{\delta}_s(\mathbf{k})\tilde{\delta}_s(\mathbf{k}')\rangle \equiv (2\pi)^3 P_s(\mathbf{k})\delta_D^3(\mathbf{k}+\mathbf{k}'), \tag{5}$$

where $\delta_D^3(\mathbf{k})$ is the Dirac delta function, the ensemble average of the estimator [Eq. (4)] is found to be an unbiased estimator of the underlying power spectrum for modes with $k \gg 1/L$:

$$\begin{aligned}\langle \hat{P}_s(\mathbf{k})\rangle &= \frac{1}{V_W}\int_{\mathbf{k}\in\mathbf{k}'}\frac{\mathrm{d}^3\mathbf{k}'}{V_{\mathbf{k}}}\int\frac{\mathrm{d}^3\mathbf{q}}{(2\pi)^3}|\tilde{W}(\mathbf{q})|^2 P_s(\mathbf{k}-\mathbf{q})\\ &\simeq \frac{1}{V_W}\int_{\mathbf{k}\in\mathbf{k}'}\frac{\mathrm{d}^3\mathbf{k}'}{V_{\mathbf{k}}}P_s(\mathbf{k})\int\frac{\mathrm{d}^3\mathbf{q}}{(2\pi)^3}|\tilde{W}(\mathbf{q})|^2\\ &\simeq \frac{P_s(\mathbf{k})}{V_W}\int_{\mathbf{k}\in\mathbf{k}'}\frac{\mathrm{d}^3\mathbf{k}'}{V_{\mathbf{k}}}\int\frac{\mathrm{d}^3\mathbf{q}}{(2\pi)^3}|\tilde{W}(\mathbf{q})|^2 = P_s(\mathbf{k}).\end{aligned} \tag{6}$$

Here we used $P_s(\mathbf{k}-\mathbf{q}) \simeq P_s(\mathbf{k})$ over the integration rage of $\mathrm{d}^3\mathbf{q}$ which the window function supports and assumed that $P_s(\mathbf{k})$ is not a rapidly varying function within the $\mathbf{k}$-bin. In addition, we used the general identity for the window function [10]:

$$\begin{aligned}V_W &= \int \mathrm{d}^3\mathbf{x}W(\mathbf{x})^n\\ &= \int\left[\prod_{a=1}^{n}\frac{\mathrm{d}^3\mathbf{q}_a}{(2\pi)^3}\tilde{W}(\mathbf{q}_a)\right](2\pi)^3\delta_D^3(\mathbf{q}_{1\ldots n}),\end{aligned} \tag{7}$$

where $\mathbf{q}_{1\ldots n} \equiv \mathbf{q}_1 + \mathbf{q}_2 + \cdots + \mathbf{q}_n$.

Similarly to Takada and Hu [10] and Akitsu *et al.* [31], we study effects of super-survey modes on the redshift-space power spectrum. The super-survey modes we focus on are the large-scale density contrast and the large-scale tide, defined in terms of the *linear* matter density fluctuation field as

$$\begin{aligned}\delta_{\mathrm{b}} &\equiv \frac{1}{V_W}\int \mathrm{d}^3\mathbf{x}W(\mathbf{x})\tilde{\delta}_{\mathrm{m}L}(\mathbf{x})\\ &= \frac{1}{V_W}\int\frac{\mathrm{d}^3\mathbf{q}}{(2\pi)^3}\tilde{\delta}_{\mathrm{m}L}(\mathbf{q})\tilde{W}(-\mathbf{q}),\\ \tau_{ij} &\equiv \frac{1}{4\pi G\bar{\rho}_{\mathrm{m}}a^2V_W}\int\mathrm{d}^3\mathbf{x}W(\mathbf{x})\left[\Phi_{,ij}(\mathbf{x}) - \frac{\delta_{ij}^K}{3}\nabla^2\Phi(\mathbf{x})\right]\\ &= \frac{1}{V_W}\int\frac{\mathrm{d}^3\mathbf{q}}{(2\pi)^3}\left(\hat{q}_i\hat{q}_j - \frac{\delta_{ij}^K}{3}\right)\tilde{\delta}_{\mathrm{m}L}(\mathbf{q})\tilde{W}(-\mathbf{q}),\end{aligned} \tag{8}$$

where $\hat{q}_i \equiv q_i/q$, $\hat{q}_i\hat{q}^i = 1$, δ_{ij}^K is the Kronecker delta, and $\Phi(\mathbf{x})$ is the gravitational potential field. Here we assumed that a survey volume is sufficiently large, and therefore the matter density field contributing the super-survey modes are in the linear regime, denoted as $\delta_{\mathrm{m}L}(\mathbf{x})$. Under this setting, $|\delta_{\mathrm{b}}|, |\tau_{ij}| \ll 1$. These super-survey modes are not direct observables and vary with survey realizations. For a particular survey realization, $\delta_{\mathrm{b}}, \tau_{ij}$ have particular constant values. The *expectation* values of the ensemble averages, i.e. the averages over different, possible survey realizations for a fixed volume, are computed if the linear matter power spectrum at long wavelengths for super-survey modes, $P^L(k)$, is given for a given cosmological model: $\langle\delta_{\mathrm{b}}\rangle = \langle\tau_{ij}\rangle = 0$, and the variances are

$$\begin{aligned}\sigma_b^2 &\equiv \langle\delta_{\mathrm{b}}^2\rangle = \frac{1}{V_W^2}\int\frac{\mathrm{d}^3\mathbf{q}}{(2\pi)^3}P^L(q)|W(\mathbf{q})|^2,\\ \langle\delta_{\mathrm{b}}\tau_{ij}\rangle &= \frac{1}{V_W^2}\int\frac{\mathrm{d}^3\mathbf{q}}{(2\pi)^3}\left(\hat{q}_i\hat{q}_j - \frac{1}{3}\delta_{ij}^K\right)P^L(q)|W(\mathbf{q})|^2,\\ \langle\tau_{ij}\tau_{lm}\rangle &= \frac{1}{V_W^2}\int\frac{\mathrm{d}^3\mathbf{q}}{(2\pi)^3}\left(\hat{q}_i\hat{q}_j - \frac{1}{3}\delta_{ij}^K\right)\left(\hat{q}_l\hat{q}_m - \frac{1}{3}\delta_{lm}^K\right)\\ &\quad\times P^L(q)|W(\mathbf{q})|^2,\end{aligned} \tag{9}$$

where $P^L(q)$ is the linear matter power spectrum.

In this paper we consider an isotropic window for simplicity; $\tilde{W}(\mathbf{q}) = \tilde{W}(q)$. In this case the variances of large-scale tide are simplified as

$$\begin{aligned}&\langle\delta_{\mathrm{b}}\tau_{ij}\rangle = 0,\\ &\sigma_\tau^2 \equiv \langle(\tau_{11})^2\rangle = \langle(\tau_{22})^2\rangle = \langle(\tau_{33})^2\rangle = \frac{3}{4}\langle(\tau_{ij})^2\rangle_{i\neq j}\\ &\quad= \frac{4}{45V_W^2}\int\frac{q^2\mathrm{d}q}{2\pi^2}P^L(q)|\tilde{W}(q)|^2 = \frac{4}{45}\sigma_{\mathrm{b}}^2.\end{aligned} \tag{10}$$

III. RESPONSES OF REDSHIFT-SPACE POWER SPECTRUM TO SUPER-SURVEY MODES

A. Redshift-space distortion effects

In a redshift galaxy survey, the radial position of each galaxy needs to be inferred from its observed redshift. Here the observed redshift can be modified by a peculiar velocity of galaxy through the Doppler effect, causing an apparent displacement of the inferred galaxy position from the true position:

$$\mathbf{s} = \mathbf{x} + \frac{v_\parallel(\mathbf{x})}{\mathcal{H}(z)}\hat{\mathbf{n}}, \tag{11}$$

where $\mathbf{s}$ is the inferred position of galaxy in redshift space, $\mathbf{x}$ is the true position in real space, $v_\parallel$ is the radial component of peculiar velocity, $\mathcal{H}(z)$ is the comoving Hubble rate, and $\hat{\mathbf{n}}$ is the unit vector of the line-of-sight direction. With this coordinate transformation, the density field in redshift space can be expressed as

$$\rho_s(\mathbf{s}) = \int \mathrm{d}^3\mathbf{x}\rho(\mathbf{x})\delta_D^3\left(\mathbf{s} - \mathbf{x} - \frac{v_\parallel(\mathbf{x})}{\mathcal{H}(z)}\hat{\mathbf{n}}\right), \tag{12}$$

where $\rho_s(\mathbf{s})$ or $\rho(\mathbf{x})$ denotes the redshift- or real-space density field of galaxies, respectively. In the following quantities with subscript "s" denote their redshift-space quantities. Fourier-transforming Eq. (12), $\int \mathrm{d}^3\mathbf{s}e^{i\mathbf{k}\cdot\mathbf{s}}$, yields

$$\delta_D^3(\mathbf{k}) + \tilde{\delta}_s(\mathbf{k}) = \int \mathrm{d}^3\mathbf{x}[1+\delta(\mathbf{x})]e^{-i\mathbf{k}\cdot\mathbf{x} - i(\mathbf{k}\cdot\hat{\mathbf{n}})\frac{v_\parallel}{\mathcal{H}}}. \tag{13}$$

This transformation is exact even if multiple galaxies are mapped to the same position in redshift space, which can happen, e.g. in a nonlinear high-density region. Such multi-streaming regions are beyond the scope of this paper, and we ignore the effects in this paper for simplicity. In this setting we can rewrite Eq. (13) as

$$\begin{aligned}\tilde{\delta}_s(\mathbf{k}) &= \int \mathrm{d}^3\mathbf{x}\left[1+\delta(\mathbf{x}) - \left|\frac{\partial s_i}{\partial x_j}\right|\right]e^{-i\mathbf{k}\cdot\mathbf{x} - i(\mathbf{k}\cdot\hat{\mathbf{n}})\frac{v_\parallel}{\mathcal{H}}} \\ &\simeq \int \mathrm{d}^3\mathbf{x}\left[\delta(\mathbf{x}) - \frac{1}{\mathcal{H}(z)}\frac{\partial v_\parallel}{\partial\hat{\mathbf{n}}}\cdot\hat{\mathbf{n}}\right]e^{-i\mathbf{k}\cdot\mathbf{x} - i(\mathbf{k}\cdot\hat{\mathbf{n}})\frac{v_\parallel}{\mathcal{H}}},\end{aligned} \tag{14}$$

where we kept the peculiar velocity up to the linear order in an expansion of the Jacobian, $|\partial s_i/\partial x_j|$, assuming $|v_\parallel/\mathcal{H}| \ll 1$.

Using the perturbation theory of structure formation [7], we can express the redshift-space density field $\tilde{\delta}_s(\mathbf{k})$ in terms of the linear matter density field $\tilde{\delta}_{\mathrm{m}L}(\mathbf{k})$ as

$$\begin{aligned}\tilde{\delta}_s(\mathbf{k};t) \equiv \sum_{n=1}^{\infty}\int\left[\prod_{a=1}^{\infty}\frac{\mathrm{d}^3\mathbf{k}_a}{(2\pi)^3}\right]Z_i(\mathbf{k}_1,\ldots,\mathbf{k}_i)\tilde{\delta}_{\mathrm{m}L}(\mathbf{k}_1,t)\cdots \\ \times\tilde{\delta}_{\mathrm{m}L}(\mathbf{k}_i,t)(2\pi)^3\delta_D^3(\mathbf{k}_{1\ldots i}-\mathbf{k})\end{aligned} \tag{15}$$

where we have introduced the notation, $\mathbf{k}_{12\ldots i} \equiv \mathbf{k}_1 + \mathbf{k}_2 + \cdots + \mathbf{k}_i$, and $Z_i(\mathbf{k}_1,\ldots,\mathbf{k}_i)$ is the mode-coupling kernel between different Fourier modes with $\mathbf{k}_1,\ldots,\mathbf{k}_i$. We throughout this paper employ a distant observer approximation for simplicity. In the following discussion we use the density fields up to the second-order, which are given as

$$\begin{aligned}\tilde{\delta}_s(\mathbf{k}) &\simeq \tilde{\delta}_s^{(1)}(\mathbf{k}) + \tilde{\delta}_s^{(2)}(\mathbf{k}) \\ &= Z_1(\mathbf{k})\tilde{\delta}_{\mathrm{m}L}(\mathbf{k}) + \int\frac{\mathrm{d}^3\mathbf{k}_1}{(2\pi)^3}\frac{\mathrm{d}^3\mathbf{k}_2}{(2\pi)^3}Z_2(\mathbf{k}_1,\mathbf{k}_2) \\ &\quad\times\tilde{\delta}_{\mathrm{m}L}(\mathbf{k}_1,t)\tilde{\delta}_{\mathrm{m}L}(\mathbf{k}_2,t)(2\pi)^3\delta_D^3(\mathbf{k}_{12}-\mathbf{k}).\end{aligned} \tag{16}$$

Using the standard Eulerian perturbation theory [42–44], where an irrotational, pressureless single-fluid matter field is assumed, the kernels are given as

$$\begin{aligned}Z_1(\mathbf{k}) &\equiv b + f\mu^2, \\ Z_2(\mathbf{k}_1,\mathbf{k}_2) &\equiv bF_2(\mathbf{k}_1,\mathbf{k}_2) + f\mu^2G_2(\mathbf{k}_1,\mathbf{k}_2) \\ &\quad + \frac{f\mu k}{2}\left[\frac{\mu_1}{k_1}(b+f\mu_2^2) + \frac{\mu_2}{k_2}(b+f\mu_1^2)\right],\end{aligned} \tag{17}$$

where $\mathbf{k} \equiv \mathbf{k}_1 + \mathbf{k}_2$, μ is the cosine angle between the wave vector $\mathbf{k}$ and the line-of-sight direction, $\mu \equiv \hat{\mathbf{n}}\cdot\hat{\mathbf{k}} = k_\parallel/k$ ($k_\parallel$ is the component along the line-of-sight direction), $f \equiv \mathrm{d}\ln D/\mathrm{d}\ln a$, D is the linear growth rate, and b is the linear bias parameter of galaxies. The pioneer work for the RSD effect is given in Ref. [36], and see Refs. [45–48] for the extension to the higher-order terms. Throughout this paper we assume the linear galaxy bias to model how the real-space distribution of galaxies is related to that of matter. Although the effect of the large-scale tide could cause an additional biasing effect on the tracers [8,49–51], the effect on the power spectrum is of the order of $\mathcal{O}((\delta_{\mathrm{m}L})^2)$, compared with the $\mathcal{O}(\delta_{\mathrm{m}L})$ effect in b, so we ignore the effect for simplicity. The kernels $F_2(\mathbf{k}_1,\mathbf{k}_2)$ and $G_2(\mathbf{k}_1,\mathbf{k}_2)$ are the second-order kernels for the density and velocity perturbations, given by Eqs. (45) and (46) in Ref. [7]:

$$\begin{aligned}F_2(\mathbf{k}_1,\mathbf{k}_2) &= \frac{5}{7} + \frac{1}{2}\left(\frac{1}{k_1^2}+\frac{1}{k_2^2}\right)(\mathbf{k}_1\cdot\mathbf{k}_2) + \frac{2}{7}\frac{(\mathbf{k}_1\cdot\mathbf{k}_2)^2}{k_1^2k_2^2}, \\ G_2(\mathbf{k}_1,\mathbf{k}_2) &= \frac{3}{7} + \frac{1}{2}\left(\frac{1}{k_1^2}+\frac{1}{k_2^2}\right)(\mathbf{k}_1\cdot\mathbf{k}_2) + \frac{4}{7}\frac{(\mathbf{k}_1\cdot\mathbf{k}_2)^2}{k_1^2k_2^2}.\end{aligned} \tag{18}$$

B. Derivation of the responses of redshift-space power spectrum to super-survey modes

We now consider how super-survey modes affect the redshift-space power spectrum observed in a finite-volume survey. Following the discussion in Refs. [10,31], in the presence of super-survey modes $(\delta_{\rm b}, \tau_{ij})$ for a given survey realization, the "observed" redshift-space power spectrum is formally expressed, up to the first order of super-survey modes, as

$$P_{sW}(\mathbf{k};\delta_{\rm b},\tau_{ij}) = P_s(\mathbf{k}) + \frac{\partial P_s(\mathbf{k})}{\partial\delta_{\rm b}}\delta_{\rm b} + \frac{\partial P_s(\mathbf{k})}{\partial\tau_{ij}}\tau_{ij}. \quad (19)$$

Here we omitted the dependence of $P_{sW}(\mathbf{k})$ on the line-of-sight direction, $\hat{\mathbf{n}}$, for notational simplicity and we explicitly denote that the observed spectrum $P_{sW}(\mathbf{k};\delta_{\rm b},\tau_{ij})$ depends on the super-survey modes of a given survey realization, and $P_s(\mathbf{k})$ is the power spectrum without the super-survey modes. The functions $\partial P_s(\mathbf{k})/\partial\delta_{\rm b}$ and $\partial P_s(\mathbf{k})/\partial\tau_{ij}$ are so-called "response" functions describing a response of the redshift-space power spectrum to the super-survey modes via mode couplings in the nonlinear structure formation. We again stress that the super-survey modes, $\delta_{\rm b}$ and τ_{ij}, are "constant" numbers for a particular survey realization. Hence, the above equation assumes that a shift in the redshift-space power spectrum due to all long-modes with wavelengths longer than a size of survey volume is described by the product of the response function and $\delta_{\rm b}$ or τ_{ij}. Furthermore, the response function is given as a function of sub-survey modes, even down to an arbitrary large k in the deeply nonlinear regime, if it is not nonvanishing. That is, we assume that, as long as the super-survey modes are in the linear regime (a survey volume is sufficiently large) and if the response function is obtained, the effects on all the small-scale modes are described by the above equation. Thus Eq. (19) rests on a nontrivial assumption, but is quite useful if Eq. (19) holds a good approximation, which is indeed the case for $\delta_{\rm b}$ as shown by many works (e.g. [22]).

Now we derive the response function using the perturbation theory. The simplest way to do this is considering a squeezed-limit bispectrum that arises from correlations between two short modes and one long mode (corresponding to super-survey modes) [52]. More specifically, let us consider a correlation of $\hat{P}_{sW}(\mathbf{k})$ [Eq. (4)] with the large-scale matter density field, $\tilde{\delta}_{{\rm m}L}(\mathbf{q})$ ($\mathbf{q}$ is the long mode):

$$\begin{aligned}\langle\hat{P}_{sW}(\mathbf{k})\tilde{\delta}_{{\rm m}L}(\mathbf{q})\rangle &= \frac{1}{V_W}\int_{\mathbf{k}'\in\mathbf{k}}\frac{{\rm d}^3\mathbf{k}'}{V_{\mathbf{k}}}\int\frac{{\rm d}^3\mathbf{q}_1}{(2\pi)^3}\frac{{\rm d}^3\mathbf{q}_2}{(2\pi)^3}\langle\tilde{\delta}_s(\mathbf{k}'-\mathbf{q}_1)\tilde{\delta}_s(-\mathbf{k}'-\mathbf{q}_2)\tilde{\delta}_{{\rm m}L}(\mathbf{q})\rangle\tilde{W}(\mathbf{q}_1)\tilde{W}(\mathbf{q}_2)\\ &= \frac{1}{V_W}\int_{\mathbf{k}'\in\mathbf{k}}\frac{{\rm d}^3\mathbf{k}'}{V_{\mathbf{k}}}\int\frac{{\rm d}^3\mathbf{q}_1}{(2\pi)^3}\frac{{\rm d}^3\mathbf{q}_2}{(2\pi)^3}B_{ss{\rm m}}(\mathbf{k}'-\mathbf{q}_1,-\mathbf{k}'-\mathbf{q}_2,\mathbf{q})(2\pi)^3\delta_D^3(\mathbf{q}_{12}-\mathbf{q})\tilde{W}(\mathbf{q}_1)\tilde{W}(\mathbf{q}_2), \quad (20)\end{aligned}$$

where we have defined the bispectrum between the redshift-space density field and the real-space density field:

$$\begin{aligned}&\langle\tilde{\delta}_s(\mathbf{k}_1)\tilde{\delta}_s(\mathbf{k}_2)\tilde{\delta}_{{\rm m}L}(\mathbf{q})\rangle\\ &\quad\equiv B_{ss{\rm m}}(\mathbf{k}_1,\mathbf{k}_2,\mathbf{q})(2\pi)^3\delta_D^3(\mathbf{k}_1+\mathbf{k}_2+\mathbf{q}). \quad (21)\end{aligned}$$

For the case that $k \gg q_1, q_2, q$, the bispectrum in the above equation arises from so-called squeezed triangles where two sides are nearly equal and in opposite direction. To see this, we can make the variable changes $\mathbf{k}-\mathbf{q}_1 \leftrightarrow \mathbf{k}$ and $\mathbf{q}_1+\mathbf{q}_2 \leftrightarrow \mathbf{q}$ under the delta function condition $\mathbf{q}_{12}+\mathbf{q}=\mathbf{0}$ and the approximation that $k \ll q$. The bispectrum we are interested in reads

$$\lim_{q\to 0} B_{ss{\rm m}}(\mathbf{k},-\mathbf{k}-\mathbf{q},\mathbf{q}). \quad (22)$$

In this limit, the triangle configuration describes how the redshift-space power spectrum $P_s(\mathbf{k})$ is modulated by the super-survey mode $\tilde{\delta}_{{\rm m}L}(\mathbf{q})$. For convenience of the following discussion, with the help of Eq. (19) we assume that the squeezed bispectrum can be described by the response of $P_s(\mathbf{k})$ to the super-survey modes as

$$\begin{aligned}&\lim_{q\to 0} B_{ss{\rm m}}(\mathbf{k},-\mathbf{k}-\mathbf{q},\mathbf{q})\\ &\quad\equiv\left[\frac{\partial P_s(\mathbf{k})}{\partial\delta_b} + \left(\hat{q}_i\hat{q}_j - \frac{\delta^K_{ij}}{3}\right)\frac{\partial P_s(\mathbf{k})}{\partial\tau_{ij}}\right]P^L(q). \quad (23)\end{aligned}$$

From Eq. (23), we can derive the response function $\partial P_s(\mathbf{k})/\partial\delta_{\rm b}$ from the angle average of the squeezed bispectrum over ${\rm d}^3\mathbf{q}$ as

$$\frac{\partial P_s(\mathbf{k})}{\partial\delta_b}P^L(q) \simeq \lim_{q\to 0}\int\frac{{\rm d}\Omega_{\mathbf{q}}}{4\pi}B_{ss{\rm m}}(\mathbf{k},-\mathbf{k}-\mathbf{q},\mathbf{q}), \quad (24)$$

With this derivation, the response to the large-scale tide, $\partial P_s(\mathbf{k})/\partial\tau_{ij}$ can be found from

$$\begin{aligned}\frac{\partial P_s(\mathbf{k})}{\partial\tau_{ij}} \leftarrow\ &\text{coefficients in}\left(\hat{q}_i\hat{q}_j - \frac{\delta^K_{ij}}{3}\right)\\ &\times P^L(q)\ \text{in}\lim_{q\to 0}B_{ss{\rm m}}(\mathbf{k},-\mathbf{k}-\mathbf{q},\mathbf{q}). \quad (25)\end{aligned}$$

Using the perturbation theory ansatz for $\tilde{\delta}_s(\mathbf{k})$ [Eq. (16)] and assuming that the large-scale mode $\tilde{\delta}_{{\rm m}L}(\mathbf{q})$ is in the

linear regime, the leading-order contribution of the squeezed bispectrum can be expressed in terms of the mode-coupling kernels as

$$B_{ssm}(\mathbf{k},-\mathbf{k}-\mathbf{q},\mathbf{q}) \simeq 2Z_1(\mathbf{k}+\mathbf{q})Z_2(\mathbf{k}+\mathbf{q},-\mathbf{q})P^L(|\mathbf{k}+\mathbf{q}|)P^L(q) + 2Z_1(\mathbf{k})Z_2(\mathbf{k},\mathbf{q})P^L(k)P^L(q). \tag{26}$$

Inserting Eq. (17) into Eq. (26) and using the relations [Eqs. (24) and (25)], we can find that the response functions for the redshift-space power spectrum are

$$\frac{\partial P_s(\mathbf{k})}{\partial \delta_b} = \left[\frac{47}{21} - \frac{1}{3}\frac{\mathrm{d}\ln P^L(k)}{\mathrm{d}\ln k}\right] b^2 P^L(k) + \left[\frac{b}{3} + \mu^2\left(\frac{26}{7}+2b\right) - \frac{\mu^2}{3}(2+b)\frac{\mathrm{d}\ln P^L(k)}{\mathrm{d}\ln k}\right] bfP^L(k)$$
$$+ \left[\frac{1}{21}(31+70b) - \frac{1}{3}(1+2b)\frac{\mathrm{d}\ln P^L(k)}{\mathrm{d}\ln k}\right] f^2\mu^4 P^L(k) + \left[\frac{1}{3}(4\mu^2-1) - \frac{\mu^2}{3}\frac{\mathrm{d}\ln P^L(k)}{\mathrm{d}\ln k}\right] f^3\mu^4 P^L(k), \tag{27}$$

and

$$\frac{\partial P_s(\mathbf{k})}{\partial \tau_{ij}} = \left[\frac{8}{7}\hat{k}_i\hat{k}_j - \hat{k}_i\hat{k}_j\frac{\mathrm{d}\ln P^L(k)}{\mathrm{d}\ln k}\right] b^2 P^L(k) + \left[b\hat{n}_i\hat{n}_j + \frac{24}{7}\mu^2\hat{k}_i\hat{k}_j - \mu(2\mu\hat{k}_i\hat{k}_j + bh_{ij})\frac{\mathrm{d}\ln P^L(k)}{\mathrm{d}\ln k}\right] bfP^L(k)$$
$$+ \left[\frac{16}{7}\mu\hat{k}_i\hat{k}_j + 4bh_{ij} - (\mu\hat{k}_i\hat{k}_j + 2bh_{ij})\frac{\mathrm{d}\ln P^L(k)}{\mathrm{d}\ln k}\right] f^2\mu^3 P^L(k) + \left[(4\mu h_{ij} - \hat{n}_i\hat{n}_j) - \mu h_{ij}\frac{\mathrm{d}\ln P^L(k)}{\mathrm{d}\ln k}\right] f^3\mu^4 P^L(k), \tag{28}$$

where

$$h_{ij} \equiv \hat{k}_{(i}\hat{n}_{j)} = \frac{1}{2}(\hat{k}_i\hat{n}_j + \hat{k}_j\hat{n}_i). \tag{29}$$

These are full expressions of the responses of redshift-space power spectrum to the large-scale perturbations. Compared with the results in Ref. [31], there are additional effects of the super-survey modes on the redshift-space power spectrum, that is, there are terms including the couplings between the large-scale tide τ_{ij} and the line-of-sight direction $\hat{\mathbf{n}}$ as expected. The response function for δ_b, $\partial P_s(\mathbf{k})/\partial\delta_b$, agrees with Eq. (65) in Ref. [53] if we set $b=1$ in the above equation. The response functions, $\partial P_s(\mathbf{k})/\partial\delta_b$ and $\partial P_s(\mathbf{k})/\partial\tau_{ij}$, show several effects caused by the super-survey modes. First, the large-scale perturbations could speed up or slow down the growth of short modes: for example, if the large-scale tide along a particular direction is positive, say $\tau_{ii}>0$, the expansion of a local volume along the direction is slower than that of the global universe, so the growth of short modes with $\mathbf{k}$ along the direction can be enhanced. Second, the super-survey modes cause a dilation of the comoving wavelengths. Because the large-scale perturbations can be realized as a modification of the local expansion, the comoving wavelengths which an observer infer are modulated by the super-survey modes, which imprints a modulation in the power spectrum. Thirdly, the super-survey modes alter the peculiar velocities through the effects on the gravitational force, so alter the redshift-space distortion effects along the line-of-sight direction. Thus the large-scale tide causes modifications in the clustering pattern along all the three directions.

In the following we focus on the response function for τ_{ij}, and we do not consider the response for δ_b. From Eq. (28) we can find several types of anisotropies in the redshift-space power spectrum: the standard RSD effect $\mu^2=\hat{k}_i\hat{k}_j\hat{n}_i\hat{n}_j$ (Kaiser factor), and the effects due to τ_{ij} that have dependences of $\tau_{ij}\hat{k}_i\hat{k}_j$, $\tau_{ij}\hat{k}_i\hat{n}_j$, and $\tau_{ij}\hat{n}_i\hat{n}_j$, respectively. First, let us remind of the physical origin of the Kaiser factor. It comes from $\partial_i v_j\hat{n}_i\hat{n}_j$ [see Eq. (14)]. This means that the Kaiser anisotropy reflects the projection of the velocity shear ($\partial_{(i}v_{j)}$, in Fourier space $\propto\hat{k}_i\hat{k}_j$) onto the line-of-sight direction. In other words, since the velocity shear corresponds to the tidal field, the Kaiser factor can be interpreted as the projection of the short-mode tidal field onto the line-of-sight direction. The terms proportional to $\tau_{ij}\hat{k}_i\hat{k}_j$ represent a coupling between the large-scale tide τ_{ij} and the small-scale tide, where the latter has directional dependences given by $\propto(\hat{k}_i\hat{k}_j-\frac{1}{3}\delta^K_{ij})$. The terms of $\tau_{ij}\hat{n}_i\hat{n}_j$ are like the Kaiser factor, that is, the projection of the large-scale tide τ_{ij} onto the line-of-sight direction. Note that the terms proportional to h_{ij} always appear with $\mu=\hat{\mathbf{k}}\cdot\hat{\mathbf{n}}$, because of the parity invariance of the power spectrum, i.e. $P_s(\mathbf{k})=P_s(-\mathbf{k})$. Then, $\tau_{ij}\hat{k}_i\hat{n}_j\mu=\tau_{ij}\hat{k}_i\hat{k}_l\hat{n}_j\hat{n}_l$ is a consequence of the projection of the coupling between the large-scale tide τ_{ij} and the small-scale velocity $\propto\hat{k}_i$ onto the line-of-sight direction.

C. The large-scale mode effects on the two-dimensional redshift-space power spectrum: $P_s^{2D}(k_\parallel,k_\perp)$

The main purpose of this paper is to estimate the impact of super-survey modes on the RSD measurements as well

as Alcock-Paczynski (AP) test [38] through a measurements of the redshift-space power spectrum. To do this, we employ the standard approach used in an analysis of the redshift-space power spectrum. Since the RSD effect is only along the line-of-sight direction and does not affect the clustering pattern in the two-dimensional plane perpendicular to the line-of-sight direction, a usual way to measure the redshift-space power spectrum is making the angle average given as

$$P^{\rm 2D}_{sW}(k_\parallel,k_\perp;\tau_{ij}) \equiv \int_0^{2\pi}\frac{{\rm d}\varphi_{\mathbf{k}_\perp}}{2\pi}P_{sW}(\mathbf{k};\tau_{ij}), \tag{30}$$

where we have set the line-of-sight direction as z-axis, $\hat{n}_i=\delta^K_{iz}$ and used the decomposition of wavevector, $\mathbf{k}=(k_\perp\cos\varphi_{\mathbf{k}_\perp},k_\perp\sin\varphi_{\mathbf{k}_\perp},k_\parallel)$ with the conditions $(k_\perp,k_\parallel)=k(\sqrt{1-\mu^2},\mu)$.

By inserting Eqs. (19) and (28) into Eq. (30) we can find

$$\begin{aligned}P^{\rm 2D}_{sW}(k_\perp,k_\parallel;\tau_{ij}) &= (b+f\mu^2)^2P^L(k)+\left[\frac{8}{7}b^2P^L(k)-b^2\frac{{\rm d}P^L(k)}{{\rm d}\ln k}\right]\frac{3\mu^2-1}{2}\tau_{33}\\ &+fb\left[\left\{b+\frac{12}{7}\mu^2(3\mu^2-1)\right\}P^L(k)-\mu^2\{b+(3\mu^2-1)\}\frac{{\rm d}P^L(k)}{{\rm d}\ln k}\right]\tau_{33}\\ &+f^2\mu^4\left[\left\{4b+\frac{8}{7}(3\mu^2-1)\right\}P^L(k)-\left(2b+\frac{3\mu^2-1}{2}\right)\frac{{\rm d}P^L(k)}{{\rm d}\ln k}\right]\tau_{33}\\ &+f^3\mu^4\left[(4\mu^2-1)P^L(k)-\mu^2\frac{{\rm d}P^L(k)}{{\rm d}\ln k}\right]\tau_{33},\end{aligned} \tag{31}$$

where we have used the following identities under the presence of the line-of-sight direction

$$\begin{aligned}\int_0^{2\pi}\frac{{\rm d}\phi_{\mathbf{k}_\perp}}{2\pi}\hat{k}_i\hat{k}_j &= \frac{1-\mu^2}{2}\delta^K_{ij}+\frac{3\mu^2-1}{2}\hat{n}_i\hat{n}_j,\\ \int_0^{2\pi}\frac{{\rm d}\phi_{\mathbf{k}_\perp}}{2\pi}\hat{k}_i &= \mu\hat{n}_i,\end{aligned} \tag{32}$$

with the traceless condition of τ_{ij}, i.e. $\tau_{ij}\delta^K_{ij}=0$. Equation (31) is one of the main results of this paper. The equation shows that the large-scale tide causes an additional anisotropic clustering in the two-dimensional redshift-space power spectrum in addition to the Kaiser distortion. The amount of the distortion depends on the line-of-sight component of the tide, τ_{33}, in a given survey realization. The tide causes anisotropic distortions up to the order of μ^6, while the standard Kaiser RSD effect causes distortions up to μ^4. Thus the large-scale tide in a given survey realization causes a bias in the redshift-space power spectrum. There are two ways to take into account the effect. One way is to include the effect as an additional noise in the error covariance matrix of the power spectrum as studied in Ref. [31]. Alternative approach, which we take in this paper, is to treat the effect as a signal rather than noise. We can model this effect by treating the bias as a purely systematic additive shift in the redshift-space power spectrum, where an amount of the bias is given by the power spectrum response multiplied by a free parameter τ_{33}. Then we can use the measured power spectrum to infer the τ_{33} value in the survey realization. We will study how a large-volume galaxy redshift survey can constrain the large-scale tide and also how it could cause a degradation in cosmological parameters.

IV. THE IMPACT OF LARGE-SCALE TIDAL EFFECT ON REDSHIFT-SPACE POWER SPECTRUM

A. Fisher information matrix

In this section, following Refs. [39,40], we study how the large-scale tide affects the BAO and RSD measurements in the redshift-space power spectrum [2], based on the Fisher information matrix formalism.

The two-point correlation function of galaxies is measured as a function of the separation lengths between paired galaxies. To measure this separation, the position of each galaxy needs to be inferred from the measured redshift and angular position. Then the separation lengths perpendicular and parallel to the line-of-sight direction from the measured quantities are given as $r_\perp\propto\Delta\theta$ and $r_\parallel\propto\Delta z$, with $\Delta\theta$ and Δz being the differences between the angular positions and the redshifts of the paired galaxies. To convert the observables $(\Delta\theta,\Delta z)$ to the quantities $(r_\perp,r_\parallel)$, one has to assume a reference cosmological model. Considering this transformation, the wave numbers are given as

$$k_{\perp,{\rm ref}}=\frac{D_A(z)}{D_{A,{\rm ref}}(z)}k_\perp,\qquad k_{\parallel,{\rm ref}}=\frac{H_{\rm ref}(z)}{H(z)}k_\parallel, \tag{33}$$

where $D_A(z)$ is the angular diameter distance and $H(z)$ is the Hubble expansion rate. The quantities with subscript "ref" mean the quantities for an assumed "reference" cosmological model, and the quantities without the

subscript mean the underlying true values. Since the reference cosmological model we assume generally differs from the underlying true cosmology, an apparent geometrical distortion is caused in the two-dimensional pattern of galaxy clustering. In principle, this distortion could be measured using only the isotropy of clustering statistics, the so-called Alcock-Paczynski (AP) test [38], but a more robust measurement of both $D_A(z)$ and $H(z)$ can be obtained by searching for the "common" BAO scales in the pattern of galaxy clustering, as the standard ruler, in combination with the CMB constraints [39,40].

We will use the currently standard ΛCDM model as a guidance for the parameter dependence of our constraints and as an effective realistic description of the galaxy clustering. To be more quantitative, we assume that the redshift-space galaxy power spectrum measured from a hypothetical survey realization is given in the linear regime as

$$P^{\rm 2D,obs}_{sW,{\rm ref}}(k_{\parallel,{\rm ref}},k_{\perp,{\rm ref}};\tau_{33})=\frac{D^2_{A,{\rm ref}}H}{D^2_A H_{\rm ref}}P^{\rm 2D}_{sW}(k_\parallel,k_\perp;\tau_{33})+P_{\rm sn}, \tag{34}$$

where $P^{\rm 2D,obs}_{sW}$ is the "observed" or "estimated" power spectrum from a given survey realization, $P^{\rm 2D}_{sW}$ on the right-hand side is the true, underlying true power spectrum [Eq. (31)], measured if an observer employs the true cosmological model, and $P_{\rm sn}$ is a parameter (constant number) to model a possible contamination of a residual shot noise to the power spectrum measurement.

To make the parameter forecast, we employ the method developed in Refs. [2,3,54]. Assuming that the redshift-space power spectrum is measured from a hypothetical survey volume the Fisher information matrix of model parameters can be computed as

$$\begin{aligned}F^{\rm galaxy}_{\alpha\beta}=&\int_{-1}^{1}{\rm d}\mu\int_{k_{\rm min}}^{k_{\rm max}}\frac{2\pi k^2{\rm d}k}{2(2\pi)^3}\frac{\partial\ln P^{\rm 2D,obs}_{sW,{\rm ref}}(k,\mu;z_i)}{\partial p_\alpha}\\&\times\frac{\partial\ln P^{\rm 2D,obs}_{sW,{\rm ref}}(k,\mu;z_i)}{\partial p_\beta}V_{\rm eff}(k;z_i)\\&\times\exp\left[-k^2\Sigma^2_\perp-k^2\mu^2(\Sigma^2_\parallel-\Sigma^2_\perp)\right],\end{aligned} \tag{35}$$

where $\partial P^{\rm 2D,obs}_{sW,{\rm ref}}/\partial p_\alpha$ is the partial derivative of the galaxy power spectrum [Eq. (34)] with respect to the α-th parameter around the reference cosmological model. The effective survey volume $V_{\rm eff}$ and the Lagrangian displacement fields $\Sigma_\parallel$ and Σ to model the smearing effect are given as

$$V_{\rm eff}(k,\mu;z_i)\equiv\left[\frac{\bar n_g(z_i)P^{\rm 2D}_{sW}(k,\mu;z_i)}{\bar n_g(z_i)P^{\rm 2D}_{sW}(k,\mu;z_i)+1}\right]^2V_{\rm survey}(z_i), \tag{36}$$

$$\Sigma_\perp(z)\equiv c_{\rm rec}D(z)\Sigma_0, \tag{37}$$

$$\Sigma_\parallel(z)\equiv c_{\rm rec}D(z)(1+f_g)\Sigma_0. \tag{38}$$

Here $V_{\rm survey}(z_i)$ is the comoving volume of the redshift slice centered at z_i, Σ_0 is the present-day Lagrangian displacement field, given as $\Sigma_0=11h^{-1}$ Mpc for $\sigma_8=0.8$ [55], and the parameter $c_{\rm rec}$ is a parameter to model the reconstruction method of the BAO peaks (see below). In Eq. (35), we take the exponential factor of the smearing effect outside of the derivatives of $P^{\rm 2D,obs}_{sW,{\rm ref}}$. This is equivalent to marginalizing over uncertainties in $\Sigma_\parallel$ and $\Sigma_\perp$. We include the parameter for the large-scale tide for the survey volume, i.e. τ_{33} in addition to the cosmological parameters, the distances in each redshift slice, and other nuisance parameters:

$$\begin{aligned}p_\alpha=\{&\tau_{33},\Omega_{\rm m0},A_s,n_s,\alpha_s,\Omega_{\rm m0}h^2,\Omega_{\rm b0}h^2,D_A(z_i),\\&H(z_i),b_g(z_i),\beta(z_i),P_{\rm sn}(z_i)\},\end{aligned} \tag{39}$$

where A_s, n_s and α_s are parameters of the primordial power spectrum; A_s is the amplitude of the primordial curvature perturbation, and n_s and α_s are the spectral tilt and the running spectral index. The set of cosmological parameters determines the shape of the linear power spectrum. For the k-integration, we set $k_{\rm min}=10^{-4}\,h/$Mpc and $k_{\rm max}=0.5\,h/$Mpc, but the exponential factor in Eq. (35) suppresses the information from the nonlinear scales. The Fisher parameter forecasts depend on the reference cosmological model for which we assumed the model consistent with the WMAP 7-year data [56]. In this paper, we consider a single redshift slice, and then consider 12 parameters in total in the Fisher analysis.

Furthermore, we assume the BAO reconstruction method in Ref. [55]. Because the large-scale peculiar velocity field of galaxies in large-scale structure can be inferred from the measured galaxy distribution, the inferred velocity field allows for pulling back each galaxy to its position at an earlier epoch and then reconstructing the galaxy distribution more in the linear regime. As a result, one can correct to some extent the smearing effect in Eq. (35) and sharpen the BAO peaks in the galaxy power spectrum. Padmanabhan *et al.* [57] implemented this method to the real data, SDSS DR7 LRG catalog, and showed that the reconstruction method can improve the distance error by a factor of 2. The improvement was equivalent to reducing the nonlinear smoothing scale from 8.1 to $\Sigma_{\rm nl}=4.4\ h^{-1}$ Mpc, about a factor of 2 reduce in the displacement field. In the Fisher matrix calculation, we used $c_{\rm rec}=0.5$ as a default choice [57].

In the following forecast, we assume the BAO experiment combined with the CMB constraints expected from the Planck satellite:

$$\boldsymbol{F}=\boldsymbol{F}^{\rm CMB}+\boldsymbol{F}^{\rm galaxy}, \tag{40}$$

where $\boldsymbol{F}_{\rm CMB}$ is the Fisher matrix for the CMB measurements. We employ the method in Ref. [2] to compute the CMB Fisher matrix, where we assumed the standard ΛCDM model for the physics prior to recombination that determines the sound horizon scale or the BAO scale.

B. Results

As a working example, we consider a hypothetical survey that is characterized by the central redshift $z = 0.5$, the comoving volume $V = 1\ (\mathrm{Gpc}/h)^3$, the mean number density of galaxies $\bar{n}_g = 10^{-3}\ (h/\mathrm{Mpc})^3$ and linear bias parameter $b = 2$, respectively. For simplicity we consider a single redshift slice. In reality, when a galaxy redshift survey probes galaxies over a wide range of redshifts, one can use the clustering analysis in multiple redshift slices and then combine their cosmological information.

In Fig. 1 we show the marginalized 68% C.L. error contours in each of two-dimensional sub-space that include either two of the large-scale tidal parameter, τ_{33}, the distance parameters, D_A or H, or the RSD parameter β, where the contours include marginalization over other parameters. Note that τ_{33} has little degeneracy with other parameters. More quantitatively, the cross-correlation coefficients defined as $c_{ij} = (F^{-1})_{ij}/\sqrt{(F^{-1})_{ii}(F^{-1})_{jj}}$ with $i = \tau_{33}$, after the CMB Fisher matrix is added, is almost unity for either one of these three parameters is taken for j, while the cross-coefficients are smaller for other parameters, less than $\mathcal{O}(0.2)$. The contours in each panel of Fig. 1 show how an uncertainty in τ_{33} causes a degeneracy with estimation of other parameter. Since the large-scale tide causes apparent anisotropies in the observed clustering of galaxies as the radial AP anisotropy and the RSD effect do, allowing τ_{33} to freely vary in the parameter estimation causes significant degeneracies with β and H. The degeneracy between τ_{33} and D_A arises from the trace-less nature of τ_{ij}; changing τ_{33} leads to a change in $\tau_{11} + \tau_{22}(= -\tau_{33})$ and therefore causes an apparent distortion in the $k_\perp$-direction, which mimics the cosmological distortion due to a change in D_A.

However, if adding the prior on τ_{33} assuming the ΛCDM model, i.e. $\tau_{33} = 0$ for the expectation value and

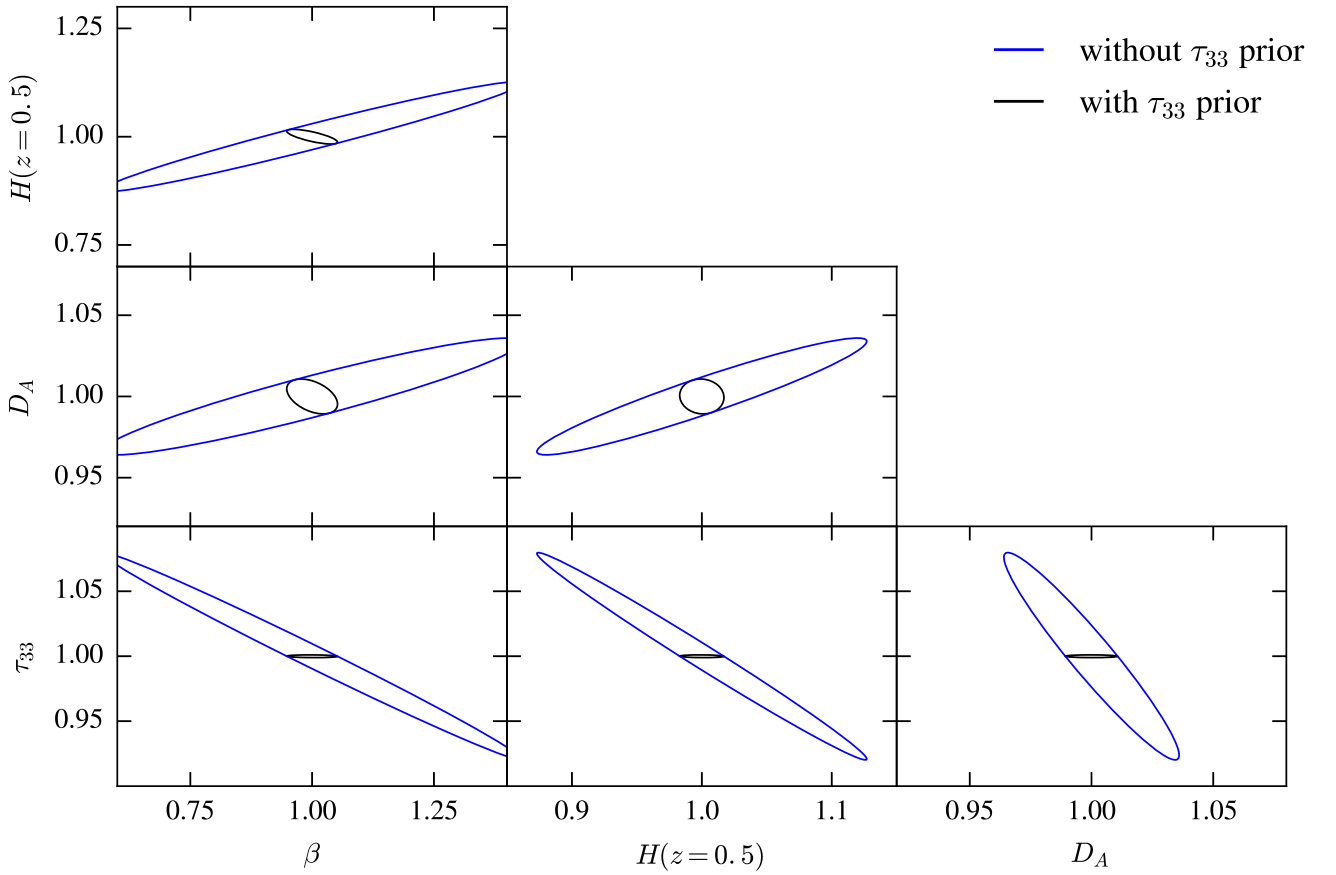

FIG. 1. 68% C.L. error ellipse for the parameters, τ_{33}, D_A, H and β, including marginalization over other parameters in the Fisher analysis (see Sec. IV A for details). The inner black contour in each panel shows the result when $\sigma_{\tau_{33}} = 1.04 \times 10^{-3}$ is employed as the τ_{33} prior, which is taken from the rms value expected for the ΛCDM model and the assumed galaxy survey that is characterized by $V = 1\ (\mathrm{Gpc}/h)^3$, $\bar{n}_{\rm g} = 10^{-3}\ (h/\mathrm{Mpc})^3$ and $b = 2$.

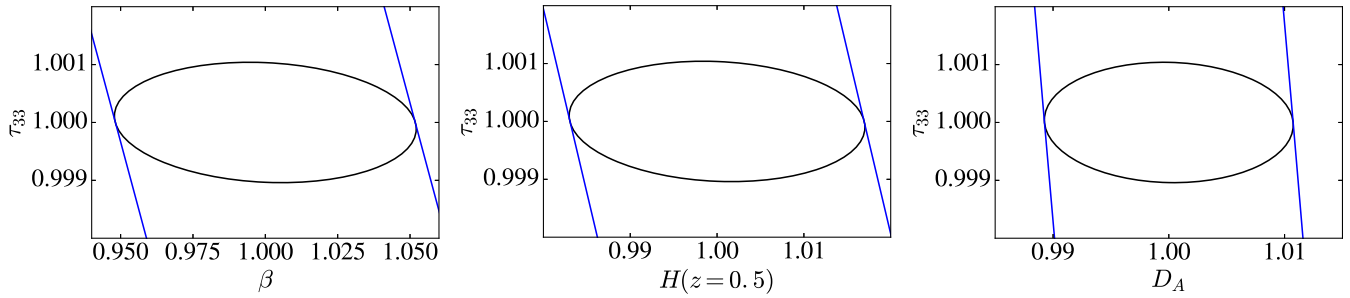

FIG. 2. A zoom-in version of Fig. 1, around the fiducial model for the Fisher analysis.

$\sigma_{\tau_{33}} = 1.04 \times 10^{-3}$ for the rms value for $V = 1\ (\mathrm{Gpc}/h)^3$, it lifts the degeneracies, recovering a high-precision measurement for each cosmological parameter. Figure 2 shows a zoomed-in version of the contours around the central value (the input model in the Fisher analysis), and shows that the prior of τ_{33} efficiently breaks the parameter degeneracies. In particular, even if an actual value of τ_{33} in a given survey realization is off from zero by more than a few $\sigma_{\tau_{33}}$, it does not seem to cause a significant bias in the parameters. It should be noted that the range of marginalized error of τ_{33} in Figs. 1 and 2 is sufficiently smaller than unity, for a hypothetical measurement of the redshift-space power spectrum for a volume of $1\ (\mathrm{Gpc}/h)^3$. Thus our assumption that the super-survey modes are in the linear regime is safely satisfied.

Nevertheless it is interesting to ask whether a measurement of redshift-shift power spectrum of galaxies can be used to constrain the large-scale tide, τ_{33}, rather than employing the prior, if one can include the information up to the larger k beyond the weakly nonlinear regime. To address this possibility, we need to know the response of the redshift-space power spectrum to the tide, $\partial P_s(\mathbf{k})/\partial\tau_{33}$, in the nonlinear regime where the perturbation theory breaks down. To estimate the response function in the nonlinear regime requires to, e.g. use a separate universe simulation where the large-scale tidal effect is included in the background expansion, similarly to the method used for estimating the response for the mean density modulation, $\partial P_s/\partial\delta_{\mathrm{b}}$, in Refs. [22,23,58,59]. This is beyond the scope of this paper, so here we simply assume that the response function derived using the perturbation theory holds in the nonlinear regime. This would be conservative, because the response is likely to be amplified in the nonlinear regime as shown in Ref. [22]. Furthermore,

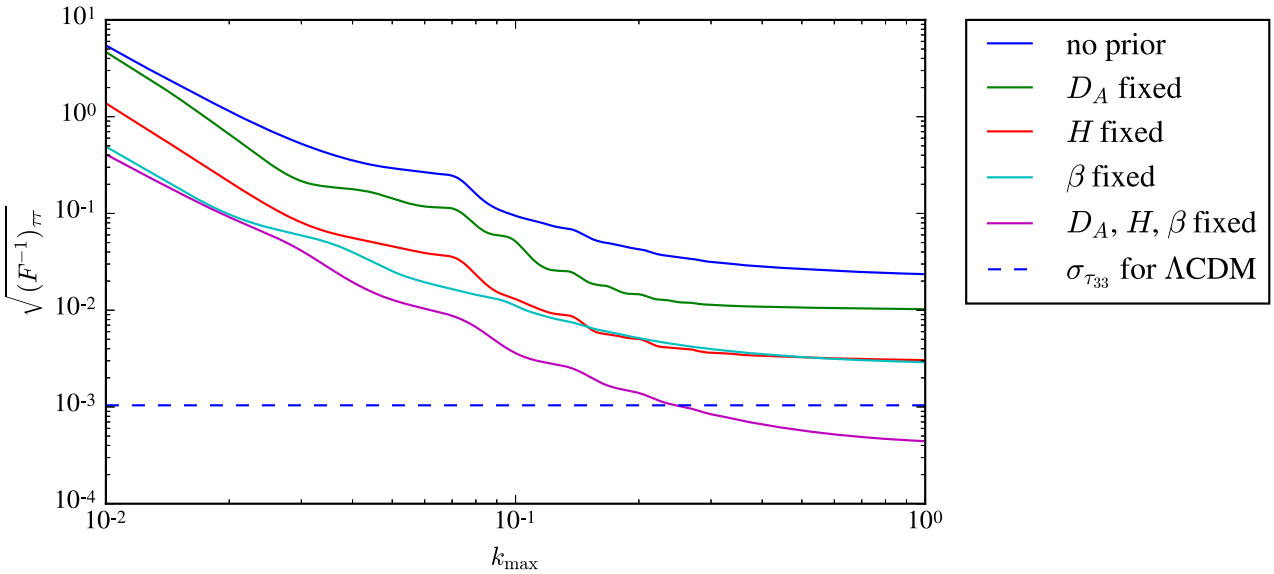

FIG. 3. The marginalized error on the estimation of τ_{33}, $\sqrt{(F^{-1})_{\tau\tau}}$, as a function of the maximum wavenumber k_{max} up to which the redshift-space power spectrum information is included in the Fisher analysis (see text for the details). The different solid curves show the results when any prior on other parameters (D_A, H and β) are not employed or when some or all the parameters are fixed to their values for the ΛCDM model. The horizontal dashed curve is the rms value, $\sigma_{\tau_{33}}$, expected for the ΛCDM model and the survey volume. Note that we did not impose any prior on other parameters [Eq. (39)], although the CMB information is added.

to include the effect of the large-scale tide up to the nonlinear regime, we set $\Sigma = 0$ for the BAO smearing factor in the Fisher analysis. In practice, the smearing factor also depends on nonlinear structure formation, and therefore would depend on τ_{33}. This is a simplified assumption, but we believe that the following result gives a rough estimation of the genuine effect. Figure 3 shows how an accuracy of the τ_{33} estimation is improved when including the redshift-space power spectrum information up to a given maximum wave number $k_{\rm max}$. Without any prior, τ_{33} is estimated to about 1% accuracy for a survey volume of $V = 1\ ({\rm Gpc}/h)^3$. When fixing other parameters to their values for ΛCDM model, the accuracy of τ_{33} is dramatically improved. In particular, when all the distortion parameters, D_A, H and β, are fixed, the τ_{33} parameter could be determined to an accuracy better than the rms for ΛCDM model, if the redshift-space power spectrum information is included up to $k_{\rm max} \gtrsim 0.25\ h/{\rm Mpc}$. This result implies that the anisotropic clustering information in such a nonlinear regime could be used to infer the large-scale tide for a given survey realization.

V. DISCUSSION

In this paper, using the standard perturbation theory, we derived the response functions of the redshift-space power spectrum to super-survey modes, both the isotropic component, $\partial P_s(\mathbf{k})/\partial\delta_{\rm b}$, and the anisotropic components, $\partial P_s(\mathbf{k})/\partial\tau_{ij}$. Since a given survey realization is generally embedded in the presence of super-survey modes, $\delta_{\rm b}$ and τ_{ij}, that are not direct observables in a finite-volume survey, it is important to take into account the response functions which describe how the super-survey modes cause a modulation in the redshift-space power spectrum measured in the survey volume, compared with the ensemble average expectation for an infinite volume. There are two effects. First, the presence of the super-survey modes changes the growth of small-scale fluctuations via the nonlinear mode coupling. Secondly, it causes a dilation effect, the modulation of a short distance scale due to the change of the local expansion factor in the finite volume region. In particular we showed that the large-scale tide, τ_{ij}, cause an apparent anisotropic clustering in the redshift-space power spectrum, where the effect has directional dependence determined by an alignment of the large-scale tide, the directions of small-scale modes, and the line-of-sight direction. This effect mimics an anisotropic clustering due to the redshift-space distortion effect of the small-scale peculiar velocities of galaxies as well as the apparent cosmological distortion caused by the use of an incorrect cosmological model in the clustering analysis.

To assess a possible impact of τ_{ij} on parameter estimation from a measurement of the redshift-space power spectrum in a given survey realization, we used the Fisher information matrix formalism. To do this, we treated the effect of τ_{ij} as a "signal" rather than an additional source of statistical errors in the redshift-space power spectrum measurement, because it causes a modulation in the measured power spectrum as do cosmological parameters around the true model: $P_s(\mathbf{k};\tau_{ij}) = P_s(\mathbf{k}) + \tau_{ij}\partial P_s(\mathbf{k})/\partial\tau_{ij}$, where the tensor τ_{ij} takes particular values in a given survey realization. Thus as long as an accurate model of the response function is given as a function of cosmological models, it would be straightforward to include the effect in parameter estimation. In this paper, we considered the two-dimensional redshift-space power spectrum, $P_s^{\rm 2D}(k_\perp, k_\parallel;\tau_{33})$ as an observable, which is obtained from the azimuthal angle average of the redshift-space power spectrum estimator in the two-dimensional plane perpendicular to the line-of-sight direction under the distant observer approximation. In this case, the effects of the large-scale tide are modeled by a single quantity, τ_{33}, the line-of-sight component of the tide. We showed that, if allowing τ_{33} to freely vary, it causes a significant degradation in the parameters, D_A, H and β, due to almost perfect degeneracies between τ_{33} and the parameters in the power spectrum. If one adopts a prior on τ_{33} assuming the rms expected for a ΛCDM model, it efficiently lifts the parameter degeneracies and restores an accuracy of the cosmological parameters that are expected for a galaxy survey without the super-survey mode. Thus the impact of the large-scale tide on the redshift-space power spectrum is not as large as the impact of the large-scale density contrast, $\delta_{\rm b}$, on a real-space power spectrum such as the weak lensing power spectrum [10,22], as long as the large-scale tide obeys the ΛCDM expectation. The reason for this less-significant impact is partly because the statistical uncertainty in a measurement of the quadrupole power spectrum, which is the lowest-order observable to extract the redshift-space distortion, is dominated by the statistical uncertainty in the monopole power spectrum measurement [31].

We have also addressed whether a measurement of redshift-space power spectrum can be used to *constrain* τ_{33} in the survey realization, rather than treating τ_{33} as a nuisance parameter. Because the presence of τ_{33} causes a mode-coupling with all the small-scale fluctuations, we showed that τ_{33} can be well constrained at an accuracy better than the rms for a ΛCDM model, if we can use the redshift-space power spectrum information up to small scales, $k_{\rm max} \gtrsim 0.25\ h/{\rm Mpc}$ and if the cosmological parameters including D_A, H and β are sufficiently well constrained, e.g. by other cosmological probes. This is an interesting possibility, because the method gives an access to such a large-scale tide from a measurement of the small-scale fluctuations, and the large-scale tide would contain the information on physics in the early universe, e.g. statistical anisotropies arising from the inflation physics [60] or a large-scale anisotropy due to the super-curvature fluctuation [61].

However, there are several limitations in the results shown in this paper. First, we used the perturbation theory prediction for the response function of redshift-space power

spectrum in the Fisher analysis, which breaks down in the deeply nonlinear regime. In order to realize the genuine functional form of the response function in the nonlinear regime, we need to use N-body simulations of large-scale structure formation and then study a coupling of the large-scale tidal modes with small-scale Fourier modes. For doing this, a "separate universe simulation" method would be powerful, where the large-scale modes are absorbed into the background expansion. It was shown that this method works very well to model the response function to the large-scale density contrast, $\partial P(k)/\partial\delta_{\rm b}$ [22,23,29,58,59,62]. To extend this method, one can adopt an anisotropic expansion background to model the effect of the anisotropic super-survey mode, τ_{ij}, and then run an N-body simulation onto the modified background (e.g., see Ref. [30] for the related discussion). If this separate universe simulation for τ_{ij} is developed, one can study various effects of τ_{ij} on nonlinear structures; the nonlocal bias of halos [50,51], the correlation between τ_{ij} and shapes of halos [63–65], and so on. This would be very interesting, and is our future work.

Another limitation of this paper is we used the redshift-space power spectrum, $P_s(k_\perp, k_\parallel)$, which is given as a function of two wave number variables such as $k_\perp$ and $k_\parallel$. Since the principle axes directions of τ_{ij} have nothing with the line-of-sight direction, the effect of τ_{ij} generally violates statistical isotropy in the two-dimensional plane perpendicular to the line-of-sight direction. Hence, in order to fully extract the three-dimensional information on the tensor τ_{ij}, one needs to use the redshift-space power spectrum given as a function of the three-dimensional vector, $P_s(\mathbf{k})$, without employing the angle average in the perpendicular plane as usually done in the standard method. Alternatively one can use a more general expansion of the redshift-space power spectrum, e.g. the bipolar spherical harmonics (BipoSH) decomposition [41,66]. It would be interesting to study how the full information on τ_{ij} can be extracted by using the BipSH decomposition.

ACKNOWLEDGMENTS

We thank Yin Li, Takahiro Nishimichi, Fabian Schmidt, Maresuke Shiraishi and Naonori Sugiyama for useful discussion, and we also thank to YITP, Kyoto University for their warm hospitality. K. A. is supported by the Advanced Leading Graduate Course for Photon Science at the University of Tokyo. M. T. is supported by World Premier International Research Center Initiative (WPI Initiative), MEXT, Japan, by the FIRST program "Subaru Measurements of Images and Redshifts (SuMIRe)", CSTP, Japan. M. T. is supported by Grant-in-Aid for Scientific Research from the JSPS Promotion of Science (No. 23340061, 26610058, and 15H05893), MEXT Grant-in-Aid for Scientific Research on Innovative Areas (No. 15K21733, 15H05892) and by JSPS Program for Advancing Strategic International Networks to Accelerate the Circulation of Talented Researchers.

APPENDIX: MULTIPOLE POWER SPECTRUM IN THE REDSHIFT-SPACE POWER SPECTRUM

Here, we show the multipole expansion of 2D power spectrum in redshift space. The multipole power spectrum are defined as

$$P_s^\ell(k;\delta_b,\tau_{33}) \equiv (2\ell+1)\int_{-1}^{1}\frac{{\rm d}\mu}{2}P_{sW}^{2D}(k,\mu;\delta_b,\tau_{33})\mathcal{L}_\ell(\mu), \tag{A1}$$

where $\mathcal{L}_\ell(\mu)$ is the Legendre polynomial. Making the use of Eqs. (27) and (31), the multipole power spectra in redshift space can be calculated as

$$\begin{aligned}P_s^{\ell=0} = {}& \left[b^2+\frac{2}{3}bf+\frac{1}{5}f^2\right]P(k)+\delta_b\left[\left\{\frac{94}{21}b^2+\frac{52}{21}bf+2b^2f+\frac{62}{105}f^2+\frac{4}{3}bf^2+\frac{26}{105}f^3\right\}P(k)\right.\\ &\left.-\left\{\frac{2}{3}b^2+2b^2f+\frac{4}{9}bf+\frac{2}{9}b^2f+\frac{2}{15}f^2+\frac{4}{15}fb^2+\frac{2}{21}f^3\right\}\frac{\partial P(k)}{\partial\ln k}\right]\\ &+\tau_{33}\left[\left\{2b^2f+\frac{32}{35}bf+\frac{128}{245}f^2+\frac{8}{5}bf^2+\frac{26}{35}f^3\right\}P(k)-\left\{\frac{8}{15}bf+\frac{2}{3}b^2f+\frac{8}{35}f^2+\frac{4}{5}bf^2+\frac{2}{7}f^3\right\}\frac{\partial P(k)}{\partial\ln k}\right]\end{aligned} \tag{A2}$$

$$\begin{aligned}P_s^{\ell=2} = {}& \left[\frac{4}{3}bf+\frac{4}{7}f^2\right]P(k)+\delta_b\left[\left\{\frac{8}{15}b^2f+\frac{104}{105}bf+\frac{16}{21}bf^2+\frac{248}{735}f^2+\frac{8}{45}f^3\right\}P(k)\right.\\ &\left.-\left\{\frac{4}{45}b^2+\frac{8}{45}bf+\frac{16}{105}bf^2+\frac{8}{105}f^2+\frac{4}{63}f^3\right\}\frac{\partial P(k)}{\partial\ln k}\right]+\tau_{33}\left[\left\{\frac{16}{35}b^2+\frac{176}{245}bf+\frac{96}{245}f^2+\frac{32}{35}bf^2+\frac{8}{15}f^3\right\}P(k)\right.\\ &\left.-\left\{\frac{2}{5}b^2+\frac{44}{105}bf+\frac{4}{15}b^2f+\frac{6}{35}f^2+\frac{16}{35}bf^2+\frac{4}{21}f^3\right\}\frac{\partial P(k)}{\partial\ln k}\right]\end{aligned} \tag{A3}$$

$$P_s^{\ell=4} = \frac{8}{35}f^2P(k) + \delta_b\left[\left\{\frac{496}{6615}f^2 + \frac{32}{189}bf^2 + \frac{112}{1485}f^3\right\}P(k) - \left\{\frac{16}{945}f^2 + \frac{32}{945}bf^2 + \frac{16}{693}f^3\right\}\frac{\partial P(k)}{\partial \ln k}\right] + \tau_{33}\left[\left\{\frac{64}{245}bf + \frac{4352}{24255}f^2 + \frac{64}{315}bf^2 + \frac{112}{495}f^3\right\}P(k) - \left\{\frac{16}{105}bf + \frac{272}{3465}f^2 + \frac{32}{315}bf^2 + \frac{16}{231}f^3\right\}\frac{\partial P(k)}{\partial \ln k}\right] \tag{A4}$$

$$P_s^{\ell=6} = \delta_b\left[\frac{128}{9009}f^3P(k) - \frac{32}{9009}f^3\frac{\partial P(k)}{\partial \ln k}\right] + \tau_{33}\left[\left\{\frac{256}{7007}f^2 + \frac{128}{3003}f^3\right\}P(k) - \left\{\frac{16}{1001}f^2 + \frac{32}{3003}f^3\right\}\frac{\partial P(k)}{\partial \ln k}\right] \tag{A5}$$

and the higher-multipole spectra with $\ell \geq 8$ vanish.

[1] M. Takada, E. Komatsu, and T. Futamase, Phys. Rev. D **73**, 083520 (2006).
[2] M. Takada *et al.*, Publ. Astron. Soc. Jpn. **66**, R1 (2014).
[3] M. Takada and O. Doré, Phys. Rev. D **92**, 123518 (2015).
[4] S. Alam *et al.*, Mon. Not. R. Astron. Soc. **470**, 2617 (2017),.
[5] S. Dodelson, *Modern Cosmology* (Academic Press, New York, 2003), p. 440 ISBN 0-12-219141-2.
[6] P. A. R. Ade, N. Aghanim, M. Arnaud, M. Ashdown, J. Aumont, C. Baccigalupi, A. J. Banday, R. B. Barreiro, J. G. Bartlett *et al.* (Planck Collaboration), Astron. Astrophys. **594**, A13 (2016).
[7] F. Bernardeau, S. Colombi, E. Gaztañaga, and R. Scoccimarro, Phys. Rep. **367**, 1 (2002).
[8] V. Desjacques, D. Jeong, and F. Schmidt, arXiv:1611.09787.
[9] M. Takada and B. Jain, Mon. Not. R. Astron. Soc. **340**, 580 (2003).
[10] M. Takada and W. Hu, Phys. Rev. D **87**, 123504 (2013).
[11] A. J. S. Hamilton, C. D. Rimes, and R. Scoccimarro, Mon. Not. R. Astron. Soc. **371**, 1188 (2006).
[12] E. Sefusatti, M. Crocce, S. Pueblas, and R. Scoccimarro, Phys. Rev. D **74**, 023522 (2006).
[13] M. Takada and S. Bridle, New J. Phys. **9**, 446 (2007).
[14] M. Takada and B. Jain, Mon. Not. R. Astron. Soc. **395**, 2065 (2009).
[15] M. Sato, T. Hamana, R. Takahashi, M. Takada, N. Yoshida, T. Matsubara, and N. Sugiyama, Astrophys. J. **701**, 945 (2009).
[16] T. Baldauf, U. Seljak, L. Senatore, and M. Zaldarriaga, J. Cosmol. Astropart. Phys. 10 (2011) 031.
[17] B. D. Sherwin and M. Zaldarriaga, Phys. Rev. D **85**, 103523 (2012).
[18] R. de Putter, C. Wagner, O. Mena, L. Verde, and W. J. Percival, J. Cosmol. Astropart. Phys. 04 (2012) 019.
[19] M. Feix and A. Nusser, J. Cosmol. Astropart. Phys. 12 (2013) 027.
[20] M. Takada and D. N. Spergel, Mon. Not. R. Astron. Soc. **441**, 2456 (2014).
[21] E. Schaan, M. Takada, and D. N. Spergel, Phys. Rev. D **90**, 123523 (2014).
[22] Y. Li, W. Hu, and M. Takada, Phys. Rev. D **89**, 083519 (2014).
[23] Y. Li, W. Hu, and M. Takada, Phys. Rev. D **90**, 103530 (2014).
[24] R. Takahashi, S. Soma, M. Takada, and I. Kayo, Mon. Not. R. Astron. Soc. **444**, 3473 (2014).
[25] A. Manzotti, W. Hu, and A. Benoit-Lévy, Phys. Rev. D **90**, 023003 (2014).
[26] J. Carron and I. Szapudi, Mon. Not. R. Astron. Soc. **447**, 671 (2015).
[27] L. Dai, E. Pajer, and F. Schmidt, J. Cosmol. Astropart. Phys. 10 (2015) 059.
[28] M. Shirasaki, M. Takada, H. Miyatake, R. Takahashi, T. Hamana, T. Nishimichi, and R. Murata, Mon. Not. R. Astron. Soc. **470**, 3476 (2017).
[29] Y. Li, W. Hu, and M. Takada, Phys. Rev. D **93**, 063507 (2016).
[30] H. Y. Ip and F. Schmidt, J. Cosmol. Astropart. Phys. 02 (2017) 025.
[31] K. Akitsu, M. Takada, and Y. Li, Phys. Rev. D **95**, 083522 (2017).
[32] A. Barreira and F. Schmidt, J. Cosmol. Astropart. Phys. 06 (2017) 053.
[33] K. C. Chan, A. Moradinezhad Dizgah, and J. Noreña, Phys. Rev. D **97**, 043532 (2018).
[34] E. Krause *et al.*, arXiv:1706.09359.
[35] F. Schmidt, E. Pajer, and M. Zaldarriaga, Phys. Rev. D **89**, 083507 (2014).
[36] N. Kaiser, Mon. Not. R. Astron. Soc. **227**, 1 (1987).
[37] A. J. S. Hamilton, in *The Evolving Universe*, Astrophysics and Space Science Library, edited by D. Hamilton (Springer, Berlin, 1998), Vol. 231, p. 185.
[38] C. Alcock and B. Paczynski, Nature (London) **281**, 358 (1979).
[39] H. Seo and D. J. Eisenstein, Astrophys. J. **598**, 720 (2003).
[40] W. Hu and Z. Haiman, Phys. Rev. D **68**, 063004 (2003).
[41] M. Shiraishi, N. S. Sugiyama, and T. Okumura, Phys. Rev. D **95**, 063508 (2017).
[42] M. H. Goroff, B. Grinstein, S.-J. Rey, and M. B. Wise, Astrophys. J. **311**, 6 (1986).

[43] N. Makino, M. Sasaki, and Y. Suto, Phys. Rev. D **46**, 585 (1992).
[44] B. Jain and E. Bertschinger, Astrophys. J. **431**, 495 (1994).
[45] E. Hivon, F. R. Bouchet, S. Colombi, and R. Juszkiewicz, Astron. Astrophys. **298**, 643 (1995).
[46] L. Verde, A. F. Heavens, S. Matarrese, and L. Moscardini, Mon. Not. R. Astron. Soc. **300**, 747 (1998).
[47] R. Scoccimarro, H. M. P. Couchman, and J. A. Frieman, Astrophys. J. **517**, 531 (1999).
[48] R. Scoccimarro, Phys. Rev. D **70**, 083007 (2004).
[49] P. McDonald and A. Roy, J. Cosmol. Astropart. Phys. 08 (2009) 020.
[50] K. C. Chan, R. Scoccimarro, and R. K. Sheth, Phys. Rev. D **85**, 083509 (2012).
[51] S. Saito, T. Baldauf, Z. Vlah, U. Seljak, T. Okumura, and P. McDonald, Phys. Rev. D **90**, 123522 (2014).
[52] C.-T. Chiang, C. Wagner, F. Schmidt, and E. Komatsu, J. Cosmol. Astropart. Phys. 05 (2014) 048.
[53] T. Nishimichi and P. Valageas, Phys. Rev. D **92**, 123510 (2015).
[54] H.-J. Seo and D. J. Eisenstein, Astrophys. J. **665**, 14 (2007).
[55] D. J. Eisenstein, H.-J. Seo, E. Sirko, and D. N. Spergel, Astrophys. J. **664**, 675 (2007).
[56] E. Komatsu *et al.*, Astrophys. J. Suppl. Ser. **192**, 18 (2011).
[57] N. Padmanabhan, X. Xu, D. J. Eisenstein, R. Scalzo, A. J. Cuesta, K. T. Mehta, and E. Kazin, Mon. Not. R. Astron. Soc. **427**, 2132 (2012).
[58] C. Wagner, F. Schmidt, C.-T. Chiang, and E. Komatsu, Mon. Not. R. Astron. Soc. **448**, L11 (2015).
[59] T. Baldauf, U. Seljak, L. Senatore, and M. Zaldarriaga, J. Cosmol. Astropart. Phys. 09 (2016) 007.
[60] D. Jeong and M. Kamionkowski, Phys. Rev. Lett. **108**, 251301 (2012).
[61] C. Byrnes, G. Domènech, M. Sasaki, and T. Takahashi, J. Cosmol. Astropart. Phys. 12 (2016) 020.
[62] W. Hu, C.-T. Chiang, Y. Li, and M. LoVerde, Phys. Rev. D **94**, 023002 (2016).
[63] N. E. Chisari, C. Dvorkin, F. Schmidt, and D. N. Spergel, Phys. Rev. D **94**, 123507 (2016).
[64] T. Okumura, T. Nishimichi, K. Umetsu, and K. Osato, arXiv:1706.08860.
[65] K. Osato, T. Nishimichi, M. Oguri, M. Takada, and T. Okumura, arXiv:1712.00094.
[66] N. S. Sugiyama, M. Shiraishi, and T. Okumura, Mon. Not. R. Astron. Soc. **473**, 2737 (2018).